

ORIGINAL ARTICLE

Novel somatic mutations in large granular lymphocytic leukemia affecting the STAT-pathway and T-cell activation

El Andersson¹, HLM Rajala¹, S Eldfors², P Ellonen², T Olson³, A Jerez⁴, MJ Clemente⁴, O Kallioniemi², K Porkka¹, C Heckman², TP Loughran Jr³, JP Maciejewski⁴ and S Mustjoki¹

T-cell large granular lymphocytic (T-LGL) leukemia is a clonal disease characterized by the expansion of mature CD3 + CD8 + cytotoxic T cells. It is often associated with autoimmune disorders and immune-mediated cytopenias. Our recent findings suggest that up to 40% of T-LGL patients harbor mutations in the *STAT3* gene, whereas *STAT5* mutations are present in 2% of patients. In order to identify putative disease-causing genetic alterations in the remaining T-LGL patients, we performed exome sequencing from three *STAT* mutation-negative patients and validated the findings in 113 large granular lymphocytic (LGL) leukemia patients. On average, 11 CD8 + LGL leukemia cell-specific high-confidence nonsynonymous somatic mutations were discovered in each patient. Interestingly, all patients had at least one mutation that affects either directly the *STAT3*-pathway (such as *PTPRT*) or T-cell activation (*BCL11B*, *SLIT2* and *NRP1*). In all three patients, the *STAT3* pathway was activated when studied by RNA expression or pSTAT3 analysis. Screening of the remaining 113 LGL leukemia patients did not reveal additional patients with same mutations. These novel mutations are potentially biologically relevant and represent rare genetic triggers for T-LGL leukemia, and are associated with similar disease phenotype as observed in patients with mutations in the *STAT3* gene.

Blood Cancer Journal (2013) 3, e168; doi:10.1038/bcj.2013.65; published online 6 December 2013

Keywords: LGL-leukemia; cytotoxic T-cells; *STAT3*; *PTPRT*

INTRODUCTION

Large granular lymphocytic (LGL) leukemia was first described in 1985 as a clonal disorder involving tissue invasion of the bone marrow, spleen and liver.¹ Patients are prone to recurrent infections and often suffer from neutropenia, anemia, splenomegaly and autoimmune diseases such as rheumatoid arthritis (RA) and systemic lupus.² LGL leukemia can be divided into T-cell and natural killer (NK)-cell LGL leukemia depending upon the type of cell that is affected. T-cell LGL (T-LGL) leukemia is characterized as a chronic leukemia where there is an expansion of CD3 + CD8 + cytotoxic T cells.

The prevalence of LGL leukemia has not yet been accurately established and it could be underdiagnosed, but it has been estimated to range from 2 to 5% of all chronic lymphoproliferative diseases in North America.³ In Western countries, LGL leukemia arising from T-cells is much more frequent (85%) than NK-cell disease (15%). T-LGL leukemia is diagnosed at a median age of 55–60 years and has an equal gender distribution. Only 20–25% of patients are younger than 50 years.³

Our recent findings suggest that up to 40% of T-LGL patients harbor mutations in the *STAT3* gene,^{4,5} whereas a smaller subset of patients present with mutations in the *STAT5B* gene.⁶ Although these findings emphasize the role of *STAT* family genes in the pathogenesis of LGL leukemia, the underlying genetic defects in the remaining T-LGL patients are yet to be discovered. In order to identify additional somatic mutations, we chose three *STAT3* and *STAT5* mutation-negative T-LGL leukemia patients for exome sequencing.

MATERIALS AND METHODS

Study patients

The study was undertaken in compliance with the principles of the Helsinki declaration and was approved by the ethics committees in the Helsinki University Central Hospital (Helsinki, Finland), the Cleveland Clinic (Cleveland, Ohio) and the Penn State Hershey Cancer Institute (Hershey, Pennsylvania). All patients and healthy controls gave written informed consents.

The patient cohort consisted of 116 LGL-leukemia patients who were confirmed to be *STAT3* and *STAT5* mutation negative by exome sequencing or amplicon sequencing. The three patients selected for exome sequencing were untreated patients who were newly diagnosed at our unit, and therefore fresh blood samples were available for sorting of CD8 + tumor and CD4 + control cells. The majority of the remaining cohort ($n = 113$) consisted of archived DNA samples or frozen cells. In total, the cohort consisted of 92 T-LGL leukemia and 24 NK-LGL leukemia cases. Forty-six samples were from the Penn State Hershey Cancer Institute, sixty-one from the Cleveland Clinic and nine from Finland. All patients met the criteria of LGL leukemia as defined by the World Health Organization in 2008.

Sample preparation

Mononuclear cells were separated from all patient samples with Ficoll-Paque PLUS (GE Healthcare, Buckinghamshire, UK). Patient samples sent for exome sequencing were further labeled with CD4 and CD8 magnetic MicroBeads (Miltenyi Biotec, San Diego, CA, USA) and separated with an AutoMACS magnetic cell sorter (Miltenyi Biotec). A small amount of the CD8 + and CD4 + cells were used to analyze and confirm the purity of the sorted fractions with flow cytometry (FACSria, Becton Dickinson, San Jose, CA, USA).

¹Department of Medicine, Hematology Research Unit Helsinki, University of Helsinki and Helsinki University Central Hospital (HUCH), Helsinki, Finland; ²Institute for Molecular Medicine Finland (FIMM), University of Helsinki, Helsinki, Finland; ³Penn State Hershey Cancer Institute, Penn State Hershey College of Medicine, Hershey, PA, USA and ⁴Translational Hematology and Oncology Research, Taussig Cancer Institute, Cleveland Clinic, Cleveland, OH, USA. Correspondence: Dr S Mustjoki, Department of Medicine, Hematology Research Unit Helsinki, University of Helsinki and Helsinki University Central Hospital, Haartmaninkatu 8, PO Box 700, Helsinki FIN-00029, Finland.

E-mail: satu.mustjoki@helsinki.fi

Received 30 October 2013; accepted 6 November 2013

DNA and RNA extraction

DNA was extracted from fresh or frozen mononuclear cell, CD8+ and CD4+ fractions with the Nucleospin Tissue Kit (Macherey-Nagel, Düren, Germany). RNA extraction from CD8+ and CD4+ fractions was performed using miRNeasy Mini kit (Qiagen, Venio, The Netherlands). DNA and RNA concentrations were measured using Qubit 2.0 Fluorometer (Invitrogen, Carlsbad, CA, USA) and NanoDrop 2000 spectrophotometer (Thermo Scientific, Wilmington, DE, USA), whereas the quality was assessed using the Agilent 2100 Bioanalyzer (Agilent Technologies, Santa Clara, CA, USA).

V β analysis

Peripheral blood samples from the three exome-sequenced T-LGL patients were used to determine the T-cell receptor (TCR) V β repertoire of human T lymphocytes with the IO Test Beta Mark TCR V β Repertoire Kit (Beckman-Coulter Immunotech, Marseille, France). The kit contains mixtures of conjugated TCR V β antibodies corresponding to 24 different specificities, covering about 70% of the normal human TCR V β repertoire. To focus on specific blood cells, the antibodies in the kit were used together with CD3+, CD4+ and CD8+ antibodies. The samples were analyzed by flow cytometry (FACSAria, Becton Dickinson) in order to detect aberrant clonal expansion.

Exome sequencing

CD8+ T cells and matched CD4+ T cells from three STAT-negative T-LGL patients were used as tumor and control samples for exome sequencing. As described previously,⁴ the exome was captured with the Nimblegen SeqCap EZ Exome Library v2.0 (Nimblegen, Basel, Switzerland) and the sequencing was performed with the Illumina HiSeq2000 sequencing platform (Illumina, San Diego, CA, USA). Candidate somatic mutations were identified with a bioinformatics pipeline consisting of Burrows-Wheeler Aligner for sequence alignment,⁷ Samtools for alignment filtering,⁸ Varscan2 for somatic mutation calling⁹ and Annovar for functional consequence prediction¹⁰ as described previously.⁴

Validation and screening of candidate somatic mutations by capillary sequencing

The candidate mutations were validated and screened by capillary sequencing in 113 STAT-mutation-negative patients. Primers were designed using Primer-Blast (<http://www.ncbi.nlm.nih.gov/tools/primer-blast/>, National Center for Biotechnology Information). Capillary PCR products were either separated by gel electrophoresis and extracted from the gel using the QIAquick Gel Extraction Kit (Qiagen) or purified using ExoSAP-IT (Affymetrix, Santa Clara, CA, USA). The purified PCR products were sequenced with BigDye v.1.1 Cycle Sequencing kit and ABI PRISM 3730xl DNA Analyzer (Applied Biosystems, Carlsbad, CA, USA). Sequences were analyzed using 4Peaks v1.7.2 (Amsterdam, The Netherlands), Sequencher v5.0.1 (Ann Arbor, MI, USA) and BLAST.

The primer sequences are listed in the Supplementary Table 1.

Immunohistochemistry (IHC)

IHC staining with pSTAT3 and CD57 antibodies was performed with Leica BOND-MAX autostainer (Leica Microsystems, Wetzlar, Germany) to detect the infiltration of LGL cells (CD57 staining) and phosphorylation of STAT3 (pSTAT3 staining). Paraffin sections from five LGL leukemia patients and two healthy control bone marrow biopsies were processed with Bond Polymer Refine Detection kit (Leica Microsystems) using citrate buffer for antigen retrieval. Staining was done with a STAT3 Tyr 705 antibody (9145L, Cell Signaling Technology, Danvers, MA, USA) diluted 1:100 or a CD57 antibody (TB01, Dako, Glostrup, Denmark) diluted 1:100.

The slides were analyzed with the Zeiss Axio Imager AX10 microscope (Zeiss, Jena, Germany) and photographed with Nuance FX multispectral tissue imaging system (420–720 nm; PerkinElmer, Waltham, MA, USA). The pictures were managed and prepared with Nuance 3.0.0 (PerkinElmer).

Microarray expression analysis

RNA was extracted from CD8+ cells of patient 1, 2 and 3 as well as from 2 STAT3-mutated LGL-patients. Anonymous Red Cross buffy coat CD4+, CD8+ and NK RNA were used as biological replicates and controls in the experiment. Microarray analysis was performed using the Illumina Human HT-12 v4 BeadChip expression array (Illumina), which targets >47 000 probes in the human genome (cover content from NCBU RefSeq Release

38 and legacy UniGene content). The data were read with an iScan instrument (Illumina) and primary analysis was done with Genome Studio software v2011.1 (Illumina). The results were normalized and log2-transformed with the Chipster open source platform.¹¹ In order to determine the similarity of the expression profiles a distance dendrogram was constructed using Pearson correlation and the average linkage method. Differentially expressed genes were filtered from the data using the empirical Bayes test with *P*-value cutoff of 0.05.

Microarray data are available in the ArrayExpress database (<http://www.ebi.ac.uk/arrayexpress>) under accession numbers E-MTAB-1611 and E-MTAB-2068.

RESULTS

Clinical characteristics

Three patients who were previously found not to carry *STAT3* or *STAT5* mutations were selected for exome sequencing. All patients suffered from T-LGL-leukemia with the phenotype CD3+ CD8+ CD57+ TCR $\alpha\beta$ + CD5dim (Figure 1a). Furthermore, all patients harbored a single monoclonal expansion, which was detected by Vbeta-analysis (Figures 1b, 2a and 3a). Two of the patients displayed a major clonal expansion (73 and 89% of CD8+ lymphocytes), whereas one patient had a smaller expansion (28%; Table 1). No clonal expansions were detected in the CD4+ lymphocytes.

In all patients, T-LGL leukemia was diagnosed at an advanced age (>60 years). Patients 1 and 2 suffered from concomitant neutropenia, whereas patient 2 also had anemia and monoclonal gammopathy of unknown significance that had not required treatment thus far. Patient 3 had no concomitant disorders (more detailed clinical characteristics can be found in Table 1).

Mutations revealed by exome sequencing

Exome sequencing of tumor (CD8+) and healthy (CD4+) cells yielded on average 53 184 000 paired reads that were mapped to the reference genome. The paired-end read length was 99 nucleotides for patient 1 and 101 for patients 2 and 3. The bioinformatics pipeline identified mutations expected to have deleterious impact on protein function based on PolyPhen predictions and conservation scores (Genomic Evolutionary Rate Profiling). On average, patients had 11 high-confidence non-synonymous mutation calls with somatic *P*-values below 0.01 (see Supplementary Table 2). The variants chosen for validation by PCR are listed in Table 2. Variants were chosen based on *P*-value, medical relevance and gene expression data from RNA sequencing when available.

Mutations affecting the STAT3 pathway

Patient 1 was diagnosed with T-LGL leukemia at the age of 70 years and the TCR repertoire assay revealed one minor T-cell clone in the peripheral blood (V β 7.1: 28%; Figure 1b). Exome sequencing of the CD8+ tumor and matched CD4+ control samples revealed 10 nonsynonymous nucleotide variants with *P*-values below 0.01. These mutations were validated by Sanger sequencing of the CD8+ tumor cells and not detected in the CD4+ healthy cell fraction. The tumor-suppressor gene protein tyrosine phosphatase (PTP) receptor T (*PTPRT*) was found to be heterozygously mutated with a variant frequency of 14%, corresponding well to the 28% clone seen in the leukemic sample (Figures 1b–d). *PTPRT* was previously found to reverse Tyr705 phosphorylation on STAT3, a modification associated with STAT3 deactivation.¹² In this novel mutation, a highly conserved hydrophobic valine residue is converted into methionine (V995M). The mutation occurs in the cytoplasmic part of the protein, within the catalytically active tyrosine-protein phosphatase 1 domain (Figure 1e). The *PTPRT* V995M mutation could therefore affect STAT3 activity by reducing dephosphorylation of Tyr705, thus increasing the expression of STAT3 target genes.

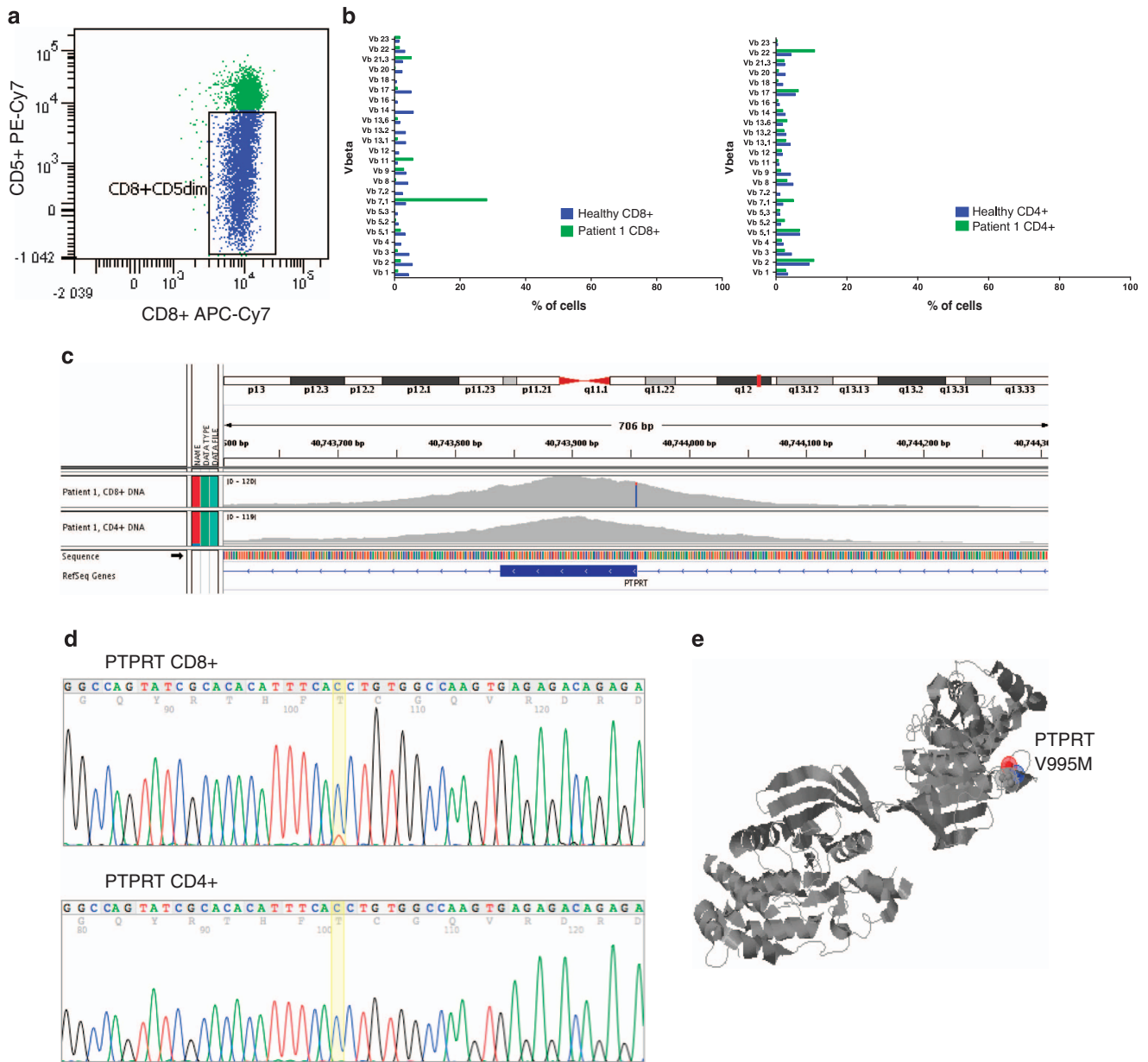


Figure 1. Flow cytometry, sequencing and V β results from patient 1. **(a)** The lymphocyte expansion of patient 1 showed typical immunophenotype of LGL cells; CD3 + CD57 + CD8 + TCR $\alpha\beta$ + CD5dim as shown by the plot. **(b)** At the time of sample collection, patient 1 presented with a minor V β .7.1 clone (28.2%) in the CD8 + population. **(c)** The somatic *PTPRT* mutation as shown by Integrative Genomics Viewer (IGV). The variant was observed in 13 reads out of a total of 92 reads with exome sequencing giving it a variant allele frequency of 14%. In the CD4 + control sample, only the normal allele was detected (66 reads). **(d)** Chromatograms from the patients selected CD8 + and CD4 + fractions showing the *PTPRT* mutation site (C > T). **(e)** Schematic representation of the location of the mutation in *PTPRT* (Polyphen2). The V995M mutation is located in the tyrosine-protein phosphatase 1 domain, which is actively responsible for the phosphatase activity of *PTPRT*. APC, allophycocyanin; Cy7, cyanine 7; M, methionine; PE, phycoerythrin; TCR $\alpha\beta$, T-cell receptor alpha and beta; V, valine.

Mutations affecting T-cell survival and activation

Patient 2 was diagnosed with LGL leukemia at the age of 76 years and harbored a major T-cell clone that constituted 73% of all CD8 + cells (Figure 2a). Exome sequencing of patient 2 revealed a H126R mutation in the *BCL11B* gene (variant frequency 51%) in the CD8 + leukemic cell fraction, but no mutation was detected in CD4 + T cells (Figures 2b and c). RNA sequencing confirmed the expression of the mutation in the CD8 + cell fraction (Table 2). *BCL11B* is required for T-cell survival and overexpression could effectively increase T-cell activation and proliferation.¹³ The *BCL11B* gene is located on chromosome 14 and is primarily

expressed in T cells, thymocytes and the brain. In hematopoietic lineages, *BCL11B* expression is restricted to T cells with transient low levels of expression in some immature NK cells. *BCL11B* has a key role in both T-cell development and maintenance of T-cell identity.¹⁴

This patient also had a missense mutation in *RAD21* (E266K), which has a role in the repair of DNA double-strand breaks as well as in chromatid cohesion in mitosis. The deletion of *RAD21* in mouse thymocytes leads to defective chromatin architecture at the TCR α locus and limited differentiation of cohesion-deficient thymocytes.¹⁵

Table 1. Clinical characteristics of the patients

Patient	LGL leukemia type	Mutations	Sex	Age at dg (years)	WBC count at dg (10E9/L)	Lymph count at dg (10E9/L)	Lymph count ^a (10E9/L)	CD8+ Vbeta ^b	Concomitant disorders	Therapy
1	CD3+ CD8+ CD57+ TCRαβ	PTPRT	F	70	7.7	6.4	3.9	Vb.7.1: 28.2%	Neutropenia, BM eosinophilia	Neutropenia: G-CSF
2	CD3+ CD8+ CD57+ TCRαβ	BCL11b	M	76	10.8	9.4	5.8	Vb.20: 73%	MGUS, neutropenia, anemia	No treatment
3	CD3+ CD8+ CD57+ TCRαβ	NRP1, SLIT2	M	60	11.1	3.7	3.8	Vb.3: 89.3%	no	No treatment

Abbreviations: BM, bone marrow; dg, diagnosis; G-CSF, granulocyte-colony stimulating factor; F, female; LGL, large granular lymphocytic; M, male; MGUS, monoclonal gammopathy of unknown significance; y, years; WBC, white blood cell. ^aLymphocyte count at the time of sample preparation. ^bProportion of Vbeta clone in CD8+ cells of the sample.

Table 2. Somatic mutations identified by exome sequencing and validated by capillary sequencing

No.	Gene	Chr	Chr. position	Mutation type	Ref. base	Var. base	Tumor variant freq.	Protein	P-value ^a	GERP ^b	RNAseq expression ^c
1	<i>PTPRT</i>	20	40743955	Missense	C	T	14.13	V995M	0.000603771	5.5	NA
	<i>LINGO2</i>	9	27949777	Missense	C	T	11.54	R298H	0.000341077	5.52	NA
2	<i>BCL11b</i>	14	99723858	Missense	T	C	51.16	H126R	1.45 ⁻⁰⁷	3.47	yes
	<i>ZC3HAV1</i>	7	138732482	Missense	G	A	37.88	T856M	3.12 ⁻¹⁶	-10.5	yes
	<i>TGS1</i>	8	56711628	Missense	T	G	38	N566K	4.62 ⁻¹⁴	-4.52	yes
	<i>RAD21</i>	8	117868903	Missense	C	T	27.12	E266K	2.45 ⁻⁰⁵	5.47	yes
3	<i>SLIT2</i>	4	20543120	Stop-gained	G	A	54.76	W674stop	6.62 ⁻⁰⁹	6.06	NA
	<i>NRP1</i>	10	33510758	Missense	C	T	37.21	V391M	1.40 ⁻⁰⁷	5.87	NA

Abbreviations: A, alanine; Chr, chromosome; E, glutamic acid; GERP, Genomic Evolutionary Rate Profiling; H, histidine; K, lysine; M, methionine; N, asparagine; NA, not available; R, arginine; Ref_base, reference base; S, serine; T, threonine; W, tryptophan; V, valine; Var_base, variant base. ^aSomatic P-value for somatic/LOH-events. ^bRejected-substitution score describing the conservation of the amino acid from the program. GERP (34 mammalian species, range of -12.3-6.17, with 6.17 being the most conserved). ^cRNA sequencing was used to analyze the expression of the mutated gene in CD8+ cells and to confirm the presence of the mutation.

Patient 3 was diagnosed with LGL-leukemia at the age of 60 years and presented with a major CD8+ clone of 89% at the time of sample collection (Figure 3a). Exome sequencing of the CD8+ LGL cells revealed a W674stop mutation in *SLIT2* with a variant frequency of 54% (Figures 3b and d). No mutation was detected in the CD4+ control fraction. The mutation is located within a cysteine-rich domain (RRCT3) bordering to a LRR-domain, which is hypothesized to mediate protein-protein interactions. *SLIT2* is a secreted glycoprotein that possesses anti-inflammatory properties. In addition, *SLIT2* has been shown to modulate CXCR4-mediated functional effects in T cells.¹⁶

Another mutation, *NRP1* V391M, was detected with a frequency of 37% in the patients' tumor sample (Figures 3c and e). The site is highly conserved and located within the Discoidin domain (F5/8 type C domain), which is a major domain of many blood coagulation factors. *NRP1* was originally known as a receptor for the semaphorin 3 subfamily mediating neuronal guidance and axonal growth. *NRP1* also binds the vascular endothelial growth factor and mediates interactions between dendritic cells (DCs) and T-cells that are essential for the initiation of the primary immune response.¹⁷

Screening of the mutations in LGL leukemia patient cohort

In order to validate the findings in a large cohort of LGL leukemia patients, we collected samples from 113 LGL leukemia patients who were *STAT3* and *STAT5* mutation negative. PCR primers were designed to cover the mutation sites of *PTPRT*, *BCL11b*, *SLIT2* and *NRP1* (Supplementary Table 1) and samples were screened with Sanger sequencing. No additional patients were found to have mutations at the tested sites.

Gene expression analysis of *STAT3* mutation-negative LGL leukemia patients

Microarray gene expression analysis was performed with CD8+ RNA from three *STAT* mutation-negative patients and two patients

with known *STAT3* mutations. CD4+, CD8+ and NK-cell fractions from healthy controls were used as biological replicates on the microarray. In the distance dendrogram based on the gene expression profile (Figure 4a), healthy CD4+, CD8+ and NK fractions clustered together, whereas LGL leukemia patients formed a separate cluster. In the LGL-leukemia cluster, patients were situated independently of *STAT* mutation status, suggesting that the expression profiles are quite similar. This was further emphasized when analyzing the differential gene expression between LGL leukemia patients with or without *STAT3* mutation: no genes were significantly over- or underexpressed. Comparison between all five LGL patients and the CD8+ healthy controls revealed 39 genes to be differentially expressed (Figure 4b). *FGR*, a member of the Src family of kinases, was overexpressed in the LGL leukemia patients when compared with healthy controls. It has been shown that *FGR*, like other Src family of kinases, can phosphorylate *STAT3* thereby activating the *STAT3* pathway.¹⁸ *FGR* is also activated by BCR-ABL in B-lymphoid cells in acute B lymphoblastic leukemia patients.¹⁹

The transmembrane receptor *SLAMF6*, which mediates important regulatory signals between immune cells through hemophilic or heterophilic interaction, was also overexpressed in LGL leukemia patients. *SLAMF6* appears to co-stimulate especially CD8+ and CD4/CD8 double-negative T cells, whereas *SLAM* signaling has also been shown to be involved in the pathogenesis of autoimmune diseases, including systemic lupus erythematosus.²⁰ Interestingly, tumor necrosis factor was expressed at a lower level in LGL leukemia patients when compared with healthy CD8+ cells.

STAT3 activation in *STAT3* mutation-negative patients

Bone marrow biopsy samples from two healthy controls and five LGL patients with different mutational status were studied with

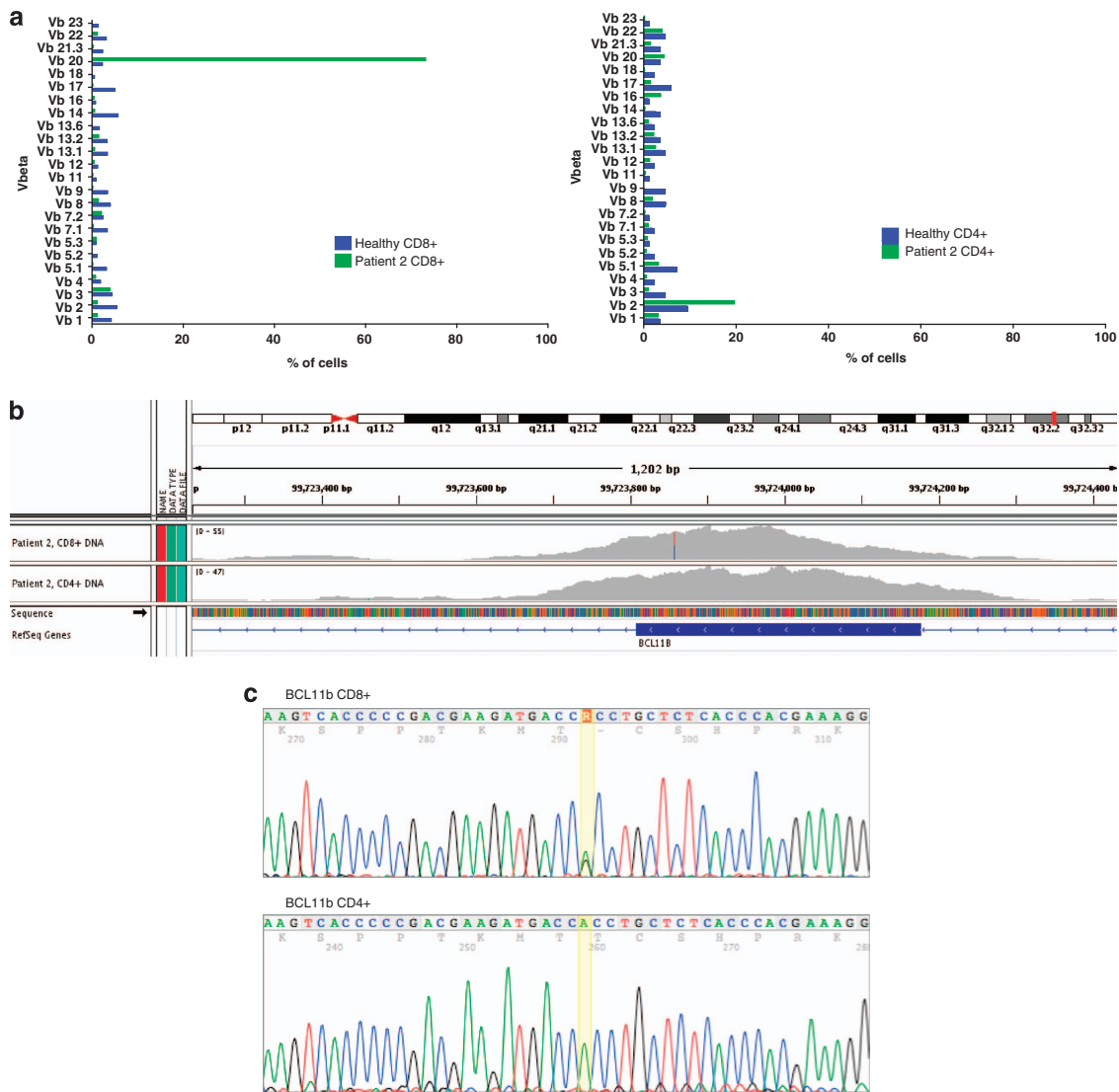


Figure 2. Sequencing and Vβ results from patient 2. **(a)** At the time of sample collection, patient 2 presented with a major Vb.20 clone (73%) in the CD8+ population. **(b)** The somatic variant H126R in *BCL11b* shown in tumor and control sample using Integrative Genomics Viewer (IGV). The variant was observed in 22 reads out of a total of 43 reads with exome sequencing giving it a variant allele frequency of 51%. In the CD4+ control sample, only the normal allele was detected (33 reads). **(c)** Chromatograms from the patients' selected CD8+ and CD4+ fractions showing the *BCL11b* mutation site (A>G). H, histidine; R, arginine.

IHC staining of CD57 and pSTAT3 expression (Figure 5). LGL cells typically express CD57 on their surface and IHC staining showed that bone marrow samples from LGL leukemia patients were infiltrated with CD57-expressing LGL cells, whereas no such infiltration was observed in bone marrow samples from healthy controls. Three of the LGL leukemia patients included in the IHC staining were *STAT* mutation positive; two patients harbored *STAT3* mutations (Y640F and D661V, Figure 5c) and one patient a *STAT5* Y665F mutation (Figure 5d). These patients presented with positive pSTAT3 staining in the infiltrated lymphocytes indicating *STAT3* activation. Phosphorylated *STAT3* was also observed in bone marrow biopsy samples of LGL patients with *PTPRT* and *BCL11B* mutations, whereas no pSTAT3 was observed in normal bone marrow. No bone marrow biopsy sample was available from patient with *SLIT2* and *NRP1* mutations.

DISCUSSION

Our previous findings showed that somatic mutations either in the *STAT3* or *STAT5* gene occur in approximately 40–50% of LGL

leukemia cases.^{4,6} However, as the *STAT3* and *STAT5* mutation-negative patients also have monoclonal expansion of LGL cells, other somatic mutations may drive these expansions. In this paper, we showed that mutations in the *PTPRT*, *BCL11B*, *SLIT2* and *NRP1* genes represent rare genetic triggers for T-LGL leukemia. These mutations are biologically relevant as they are connected either to the *STAT3* pathway or T-cell activation and proliferation.

Previous studies have shown that almost all LGL leukemia patients exhibit activation of *STAT3*, indicating that this pathway is essential for the pathogenesis of LGL leukemia.^{21,22} We recently confirmed that also LGL leukemia patients without *STAT3* mutations have activation of *STAT3* responsive genes.⁴ Similarly, in this study, we showed that *STAT3* was also phosphorylated in LGL patients without actual *STAT3* mutations, and that LGL leukemia patients clustered closely together in the RNA expression analysis independently of their mutational status. Therefore, the novel V995M mutation in the *PTPRT* gene is particularly interesting as it may directly impact the *STAT3* pathway. The mutation was found within the phosphatase domain D1 that is actively responsible for the phosphatase activity of type IIb members.

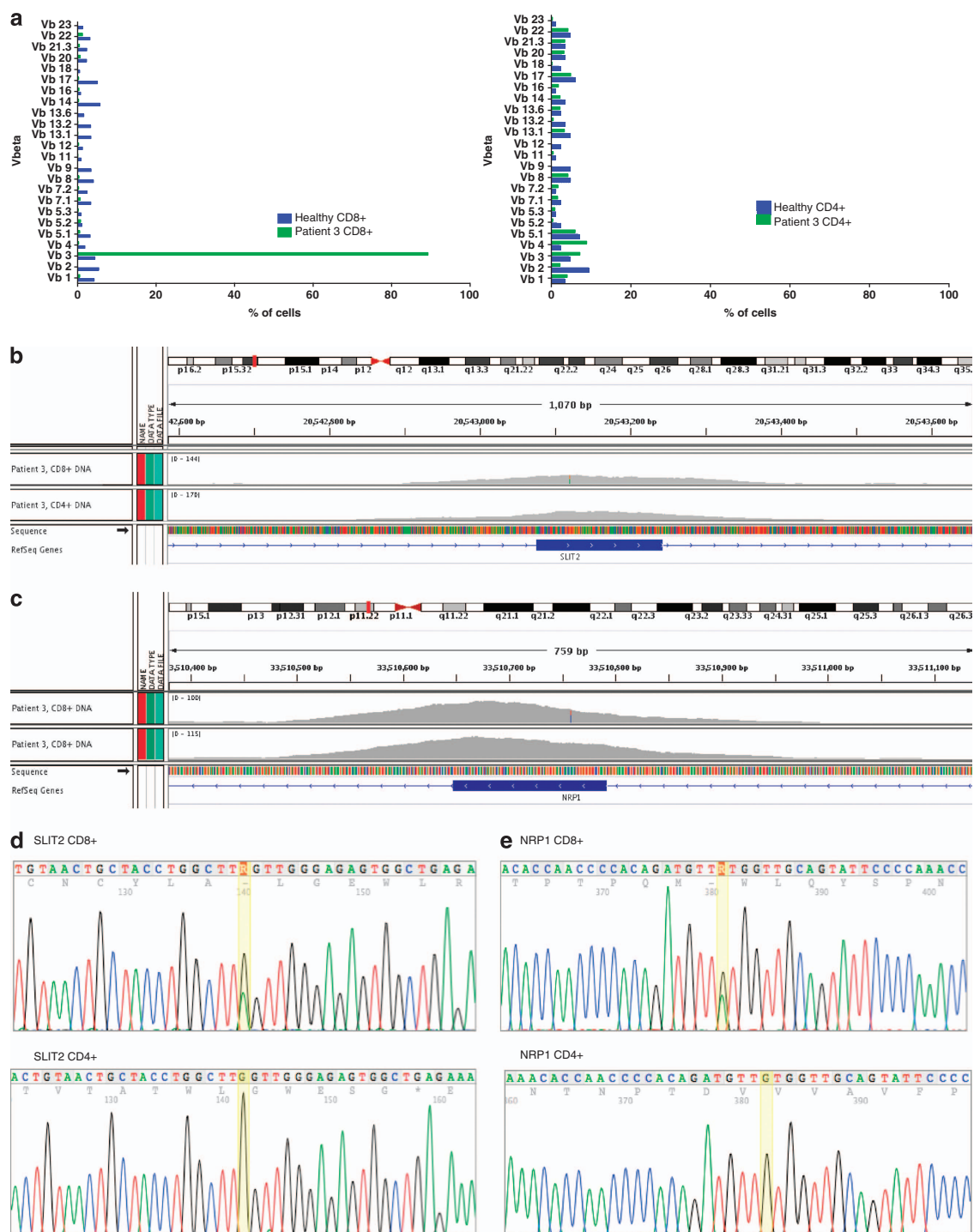


Figure 3. Sequencing and vbeta results from patient 3. **(a)** At the time of sample collection, patient 3 presented with a major Vb.3 clone (89.3%) in the CD8⁺ population. **(b)** Somatic variant in *SLIT2* shown in tumor and control sample using Integrated Genomics Viewer (IGV). The variant was observed in 19 reads out of a total of 42 reads with exome sequencing giving it a variant allele frequency of 34%. **(c)** Somatic variant in *NRP1* shown in tumor and control sample using IGV. The variant was observed in 16 reads out of a total of 43 reads with exome sequencing giving it a variant allele frequency of 34%. In the CD4⁺ control sample, only the normal allele was detected (59 reads). **(d)** Chromatograms from the patients selected CD8⁺ and CD4⁺ fractions showing the *SLIT2* mutation site (G>A). **(e)** Chromatograms from the patients selected CD8⁺ and CD4⁺ fractions showing the *NRP1* mutation site (G>A).

The *PTPRT* gene encoding PTP ρ is also frequently mutated in other cancers such as in lung and gastric cancer.²³

Pasquo *et al.*²⁴ previously studied the effect of missense mutations (D927G, Q987K, A1118P and N1128I) in the D1 domain on PTPRT stability and activation. All the mutants showed a decrease in thermal stability and activation energy for

phosphatase activity with respect to the wild-type protein. At 37°C, the phosphatase activity of all the variants was significantly reduced and the most destabilizing mutation, D927G, yielded a protein that at physiological temperature was almost completely inactive. We therefore hypothesize that inactivating mutations of the *PTPRT* gene may have the same

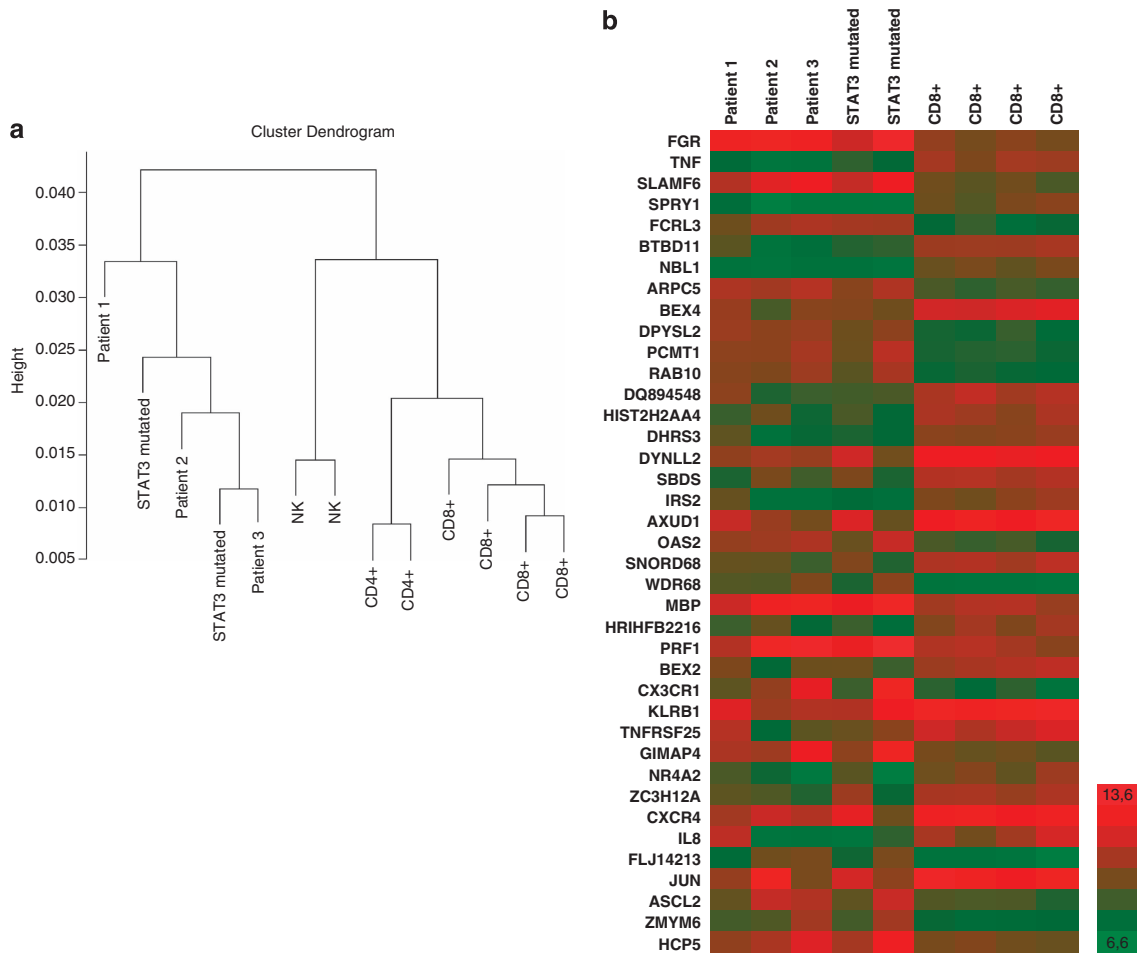


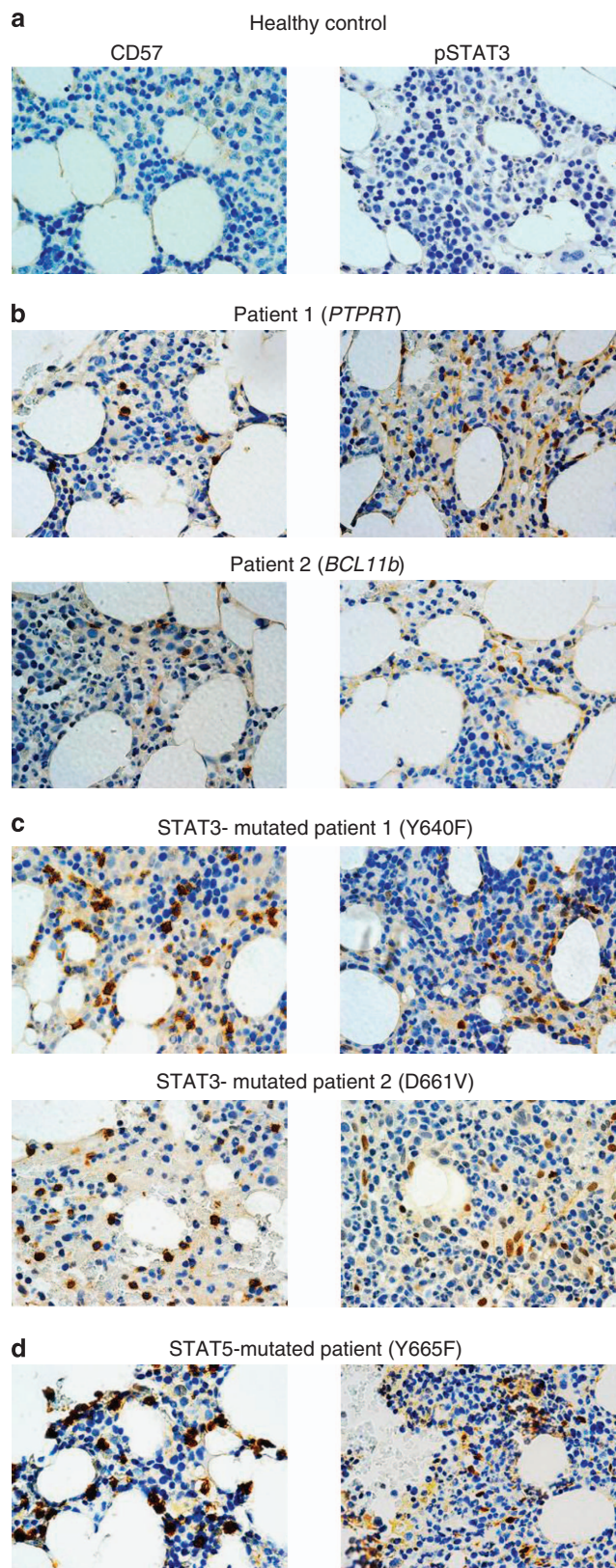
Figure 4. RNA expression data. **(a)** Distance dendrogram visualizing the clustering of LGL leukemia patients and healthy controls (NK, CD4+ and CD8+ cells) based on their gene expression profiles. **(b)** Heatmap representing the gene expression profiles of three patients without STAT mutations, two STAT3 mutated patients and four healthy controls (CD8+). A total of 39 genes were differentially expressed when comparing the LGL leukemia patients to the healthy controls ($P < 0.05$).

functional consequence as activating mutations of *STAT3* in LGL leukemia patients. Furthermore, *PTPRT* was previously found to reverse Tyr705 phosphorylation on *STAT3*, a modification associated with *STAT3* deactivation.¹² The *PTPRT* V995M mutation may thereby affect *STAT3* activity by reducing dephosphorylation of Tyr705, thus increasing the expression of *STAT3* target genes. This is in accordance with our results showing that patient 1 with the *PTPRT* mutation had increased phosphorylation of *STAT3* and activation of *STAT3* responsive genes.

In order to clonally expand, T cells must have acquired a survival advantage. It has been shown that some LGL leukemia patients have resistance to FAS-mediated apoptosis, which could be mediated through *STAT3* activation.²⁵ However, in addition to defects in apoptotic pathways, survival pathways such as PI3K-AKT may be activated in LGL leukemia patients.²¹ Therefore, it was of interest to observe that one T-LGL leukemia patient harbored a novel missense mutation H126R in the *BCL11B* gene. *BCL11B* functions as a transcription factor that is required for normal T-cell development. Inactivation of *BCL11B* in murine thymocytes leads to developmental arrest at the DN2-DN3 stage and aberrant self-renewal activity.^{26,27} The role of *BCL11B* in the pathogenesis of hematological diseases still remains controversial. Increased levels of *BCL11B* expression have been found to be associated with human T-cell acute lymphoblastic leukemia (T-ALL),²⁸ and the inhibition of *BCL11B* expression in malignant T cells results in

apoptosis.²⁹ Downregulation of *BCL11B* gene expression by small interfering RNA led to growth inhibition and apoptosis in a human T-ALL cell line, although not in normal mature T and CD34+ cells.³⁰ Furthermore, *BCL11B* knockdown in Jurkat cells induces apoptosis, whereas *BCL11B* overexpression in Jurkat cells induces cell cycle arrest under genotoxic stress, which is consistent with the oncogenic properties of *BCL11B*.^{29,31} Mutations in *BCL11B* have been reported in two separate studies of T-ALL patients; missense mutations and deletions were found in 9% of 117 unselected T-ALL patients²² and in 16% of 71 *TLX1*-overexpressing T-ALL cases.^{32,33} In addition to *BCL11B* mutation, same patient also had a mutation in the *RAD21* gene in the CD8+ fraction. *RAD21* has previously been found to be mutated in AML with a prevalence of 4.1% (7/170). In AML, the mutations were distributed over the whole gene and consisted of missense, nonsense and synonymous variants.³⁴

SLIT2 belongs to a group of large secreted glycoproteins originally described in regulating neural migration.³⁵ However, its predominant receptor Robo1 belongs to a novel subfamily of immunoglobulin superfamily proteins³⁶ and is also expressed in several nonneuronal tissues, including leukocytes. It has also been shown that *SLIT2* can inhibit T-cell chemotaxis induced by chemotactic factors through chemokine receptors CXCL12/CXCR4.¹⁶ According to COSMIC, mutations in *SLIT2* have never been found in hematopoietic or lymphoid tissues before, making the stop-gained mutation W674stop unique in this aspect.



Previously, *SLIT2* has been found frequently methylated in lung, breast, colorectal and glial tumors and it has been shown that *SLIT2* can act as a tumor-suppressor gene in breast and colorectal cancer cells.³⁷ Dunwell *et al.*³⁸ demonstrated frequent *SLIT2* methylation in hematologic malignancies (both chronic



Figure 5. Immunohistochemical staining of bone marrow-biopsy samples. Bone marrow-biopsy samples from a healthy control and five LGL leukemia patients were stained with CD57 and pSTAT3 antibodies. (a) Healthy control, (b) patients without STAT-mutations, (c) patients with STAT3 mutations and (d) patient with STAT5 mutation. No staining was observed in the healthy control, whereas the leukemic samples showed infiltration of lymphocytes positive for CD57 and pSTAT3 (magnification, $\times 63$). D, aspartic acid; F, phenylalanine; V, valine; Y, tyrosine.

lymphocytic leukemia and acute lymphoblastic leukemia), hence providing further evidence to support a role for *SLIT2* in cancer development.

NRP1, a receptor involved in axon guidance, is also expressed in human DCs and resting T cells.¹⁷ Interestingly, earlier studies have shown that NRP1 can have a role in the primary immune response during the formation of immunological synapse between DCs and resting T cells. The preincubation of DCs, but also of resting T cells with blocking NRP1 antibodies inhibited the DC-induced proliferation of T cells. Thus, the mutation in *NRP1* gene may affect the activation status or proliferation capacity of T cells.

These novel mutations affecting either the STAT3 or the T-cell activation pathway were not detected in additional patients in our screening cohort ($n = 113$). It could be that the STAT3/STAT5 mutation-negative patients are a more heterogeneous patient cohort, and therefore no similar dominant mutations (such as STAT3) will be found in this group. However, in the screening assays, the primers covered only the mutation spots and nearby base pairs, and it is possible that by screening the whole genes, some additional mutations in the same genes will be found. Especially, inactivating mutations in *PTPRT* warrant more extensive sequencing of the whole *PTPRT* gene as these mutations, unlike activating mutations in *STAT3*, do not cluster in hotspots.

In conclusion, somatic mutations in *PTPRT*, *BCL11B*, *SLIT2* and *NRP1* represent potential genetic cause for LGL leukemia. The similarities in the gene expression profile and the observation of STAT3 phosphorylation in the bone marrow biopsy samples of patients without *STAT3* mutations suggest that the novel LGL leukemia-associated mutations lead to the activation of STAT3 pathway and to similar disease phenotype as seen in patients with actual activating *STAT3* mutations.

CONFLICT OF INTEREST

H.L.M.R. has received honoraria from Novartis. K.P. has received research funding and honoraria from Novartis and Bristol-Myers Squibb. S.M. has received honoraria from Novartis and Bristol-Myers Squibb.

ACKNOWLEDGEMENTS

This work was supported by the Academy of Finland, the Finnish Cancer Societies, Sigrid Juselius Foundation, European Regional Development Fund, Swedish Cultural Foundation, Blood Disease Foundation, Medicinska Understödsföreningen Liv och Hälsa r.f and the Finnish Cultural Foundation. Work of J.P.M. and M.J.C. was supported in part by the National Institutes for Health (grants 2K24HL077522, R01 CA127264A and R01AI085578). Personnel at the Hematology Research Unit Helsinki and FIMM are acknowledged for their expert clinical and technical assistance.

AUTHOR CONTRIBUTIONS

EIA and SM designed the study, coordinated the project, analyzed the data and wrote the paper. EIA, HLMR and PE performed sequence analysis and validated mutations. SE designed and performed bioinformatics analysis. TO, AJ and MJC provided patient samples and participated in the laboratory studies. KP, CH OK, JPM and TPL participated in the study design, data analysis and contributed to write the paper. All authors read and approved the final manuscript.

REFERENCES

- Loughran Jr TP, Kadin ME, Starkebaum G, Abkowitz JL, Clark EA, Distche C *et al*. Leukemia of large granular lymphocytes: association with clonal chromosomal abnormalities and autoimmune neutropenia, thrombocytopenia, and hemolytic anemia. *Ann Intern Med* 1985; **102**: 169–175.
- Sokol L, Loughran TP Jr. Large granular lymphocyte leukemia. *Curr Hematol Malig Rep* 2007; **2**: 278–282.
- Lamy T, Loughran TP Jr. How I treat LGL leukemia. *Blood* 2011; **117**: 2764–2774.
- Koskela HL, Eldfors S, Ellonen P, van Adrichem AJ, Kuusanmaki H, Andersson El *et al*. Somatic STAT3 mutations in large granular lymphocytic leukemia. *N Engl J Med* 2012; **366**: 1905–1913.
- Jerez A, Clemente MJ, Makishima H, Koskela H, Leblanc F, Peng NgK *et al*. STAT3 mutations unify the pathogenesis of chronic lymphoproliferative disorders of NK cells and T-cell large granular lymphocyte leukemia. *Blood* 2012; **120**: 3048–3057.
- Rajala HL, Eldfors S, Kuusanmaki H, van Adrichem AJ, Olson T, Lagstrom S *et al*. Discovery of somatic STAT5b mutations in large granular lymphocytic leukemia. *Blood* 2013; **121**: 4541–4550.
- Li H, Durbin R. Fast and accurate short read alignment with Burrows-Wheeler transform. *Bioinformatics* 2009; **25**: 1754–1760.
- Li H, Handsaker B, Wysoker A, Fennell T, Ruan J, Homer N *et al*. The Sequence Alignment/Map format and SAMtools. *Bioinformatics* 2009; **25**: 2078–2079.
- Koboldt DC, Zhang Q, Larson DE, Shen D, McLellan MD, Lin L *et al*. VarScan 2: somatic mutation and copy number alteration discovery in cancer by exome sequencing. *Genome Res* 2012; **22**: 568–576.
- Wang K, Li M, Hakonarson H. ANNOVAR: functional annotation of genetic variants from high-throughput sequencing data. *Nucleic Acids Res* 2010; **38**: e164.
- Kallio MA, Tuimala JT, Hupponen T, Klemela P, Gentile M, Scheinin I *et al*. Chipster: user-friendly analysis software for microarray and other high-throughput data. *BMC Genomics* 2011; **12**: 507.
- Zhang X, Guo A, Yu J, Possemato A, Chen Y, Zheng W *et al*. Identification of STAT3 as a substrate of receptor protein tyrosine phosphatase T. *Proc Natl Acad Sci USA* 2007; **104**: 4060–4064.
- Huang X, Du X, Li Y. The role of BCL11B in hematological malignancy. *Exp Hematol Oncol* 2012; **1**: 22.
- Liu P, Li P, Burke S. Critical roles of Bcl11b in T-cell development and maintenance of T-cell identity. *Immunol Rev* 2010; **238**: 138–149.
- Seitan VC, Hao B, Tachibana-Konwalski K, Lavagnoli T, Mira-Bontenbal H, Brown KE *et al*. A role for cohesin in T-cell-receptor rearrangement and thymocyte differentiation. *Nature* 2011; **476**: 467–471.
- Wu JY, Feng L, Park HT, Havlioglu N, Wen L, Tang H *et al*. The neuronal repellent Slit inhibits leukocyte chemotaxis induced by chemotactic factors. *Nature* 2001; **410**: 948–952.
- Tordjman R, Lepelletier Y, Lemarchandel V, Cambot M, Gaulard P, Hermine O *et al*. A neuronal receptor, neuropilin-1, is essential for the initiation of the primary immune response. *Nat Immunol* 2002; **3**: 477–482.
- Schreiner SJ, Schiavone AP, Smithgall TE. Activation of STAT3 by the Src family kinase Hck requires a functional SH3 domain. *J Biol Chem* 2002; **277**: 45680–45687.
- Hu Y, Liu Y, Pelletier S, Buchdunger E, Warmuth M, Fabbro D *et al*. Requirement of Src kinases Lyn, Hck and Fgr for BCR-ABL1-induced B-lymphoblastic leukemia but not chronic myeloid leukemia. *Nat Genetics* 2004; **36**: 453–461.
- Chatterjee M, Kis-Toth K, Thai TH, Terhorst C, Tsokos GC. SLAMF6-driven co-stimulation of human peripheral T cells is defective in SLE T cells. *Autoimmunity* 2011; **44**: 211–218.
- Schade AE, Wlodarski MW, Maciejewski JP. Pathophysiology defined by altered signal transduction pathways: the role of JAK-STAT and PI3K signaling in leukemic large granular lymphocytes. *Cell Cycle* 2006; **5**: 2571–2574.
- Epling-Burnette PK, Liu JH, Catlett-Falcone R, Turkson J, Oshiro M, Kothapalli R *et al*. Inhibition of STAT3 signaling leads to apoptosis of leukemic large granular lymphocytes and decreased Mcl-1 expression. *J Clin Invest* 2001; **107**: 351–362.
- Wang Z, Shen D, Parsons DW, Bardelli A, Sager J, Szabo S *et al*. Mutational analysis of the tyrosine phosphatome in colorectal cancers. *Science* 2004; **304**: 1164–1166.
- Pasquo A, Consalvi V, Knapp S, Alfano I, Ardini M, Stefanini S *et al*. Structural stability of human protein tyrosine phosphatase rho catalytic domain: effect of point mutations. *PLoS One* 2012; **7**: e32555.
- Lamy T, Liu JH, Landowski TH, Dalton WS, Loughran TP Jr. Dysregulation of CD95/CD95 ligand-apoptotic pathway in CD3(+) large granular lymphocyte leukemia. *Blood* 1998; **92**: 4771–4777.
- Li L, Leid M, Rothenberg EV. An early T cell lineage commitment checkpoint dependent on the transcription factor Bcl11b. *Science* 2010; **329**: 89–93.
- Ikawa T, Hirose S, Masuda K, Kakugawa K, Satoh R, Shibano-Satoh A *et al*. An essential developmental checkpoint for production of the T cell lineage. *Science* 2010; **329**: 93–96.
- Oshiro A, Tagawa H, Ohshima K, Karube K, Uike N, Tashiro Y *et al*. Identification of subtype-specific genomic alterations in aggressive adult T-cell leukemia/lymphoma. *Blood* 2006; **107**: 4500–4507.
- Grabarczyk P, Przybylski GK, Depke M, Volker U, Bahr J, Assmus K *et al*. Inhibition of BCL11B expression leads to apoptosis of malignant but not normal mature T cells. *Oncogene* 2007; **26**: 3797–3810.
- Huang X, Chen S, Shen Q, Chen S, Yang L, Grabarczyk P *et al*. Down regulation of BCL11B expression inhibits proliferation and induces apoptosis in malignant T cells by BCL11B-935-siRNA. *Hematology* 2011; **16**: 236–242.
- Grabarczyk P, Nahse V, Delin M, Przybylski G, Depke M, Hildebrandt P *et al*. Increased expression of bcl11b leads to chemoresistance accompanied by G1 accumulation. *PLoS One* 2010; **5**: e12532.
- Gutierrez A, Kentsis A, Sanda T, Holmfeldt L, Chen SC, Zhang J *et al*. The BCL11B tumor suppressor is mutated across the major molecular subtypes of T-cell acute lymphoblastic leukemia. *Blood* 2011; **118**: 4169–4173.
- De Keersmaecker K, Real PJ, Gatta GD, Palomero T, Sulis ML, Tosello V *et al*. The TLX1 oncogene drives aneuploidy in T cell transformation. *Nat Med* 2010; **16**: 1321–1327.
- Dolnik A, Engelmann JC, Scharfenberger-Schmeer M, Mauch J, Kelkenberg-Schade S, Haldemann B *et al*. Commonly altered genomic regions in acute myeloid leukemia are enriched for somatic mutations involved in chromatin remodeling and splicing. *Blood* 2012; **120**: e83–e92.
- Yuan W, Zhou L, Chen JH, Wu JY, Rao Y, Ornitz DM. The mouse SLIT family: secreted ligands for ROBO expressed in patterns that suggest a role in morphogenesis and axon guidance. *Dev Biol* 1999; **212**: 290–306.
- Howitt JA, Clout NJ, Hohenester E. Binding site for Robo receptors revealed by dissection of the leucine-rich repeat region of Slit. *EMBO J* 2004; **23**: 4406–4412.
- Dallol A, Da Silva NF, Viacava P, Minna JD, Bieche I, Maher ER *et al*. SLIT2, a human homologue of the Drosophila Slit2 gene, has tumor suppressor activity and is frequently inactivated in lung and breast cancers. *Cancer Res* 2002; **62**: 5874–5880.
- Dunwell TL, Dickinson RE, Stankovic T, Dallol A, Weston V, Austen B *et al*. Frequent epigenetic inactivation of the SLIT2 gene in chronic and acute lymphocytic leukemia. *Epigenetics* 2009; **4**: 265–269.



This work is licensed under a Creative Commons Attribution-NonCommercial-NoDerivs 3.0 Unported License. To view a copy of this license, visit <http://creativecommons.org/licenses/by-nc-nd/3.0/>

Supplementary Information accompanies this paper on Blood Cancer Journal website (<http://www.nature.com/bcj>)